A scattering model for surface-textured thin films

Klaus Jäger[a)] and Miro Zeman
Photovoltaic Materials and Devices Laboratory / DIMES, Delft University of Technology, P. O. Box 5031, 2600 GA Delft, The Netherlands

(Received 3 September 2009; accepted 2 October 2009; published online 29 October 2009)

We present a mathematical model that relates the surface morphology of randomly surface-textured thin films with the intensity distribution of scattered light. The model is based on the first order Born approximation [see e.g., M. Born and E. Wolf, *Principles of Optics*, 7th ed. (Cambridge University Press, Cambridge, England, 1999)] and on Fraunhofer scattering. Scattering data of four transparent conductive oxide films with different surface textures were used to validate the model and good agreement between the experimental and calculated intensity distribution was obtained. © *2009 American Institute of Physics*. [doi:10.1063/1.3254239]

To enhance the energy conversion efficiency of thin-film silicon solar cells, light trapping is commonly used in order to increase the absorption of light in the absorber layers. Light trapping is based on refractive-index matching layers, highly reflective back contacts, and scattering of light at rough interfaces inside the solar cell.[1] Scattering at rough interfaces leads to a longer average photon path length inside the absorber layer and partially to total internal reflection between the back and front contacts confining the light inside the absorber. These two effects lead to an increased absorption, resulting in a higher photocurrent.

The rough interfaces are usually introduced into the solar cells by using substrate carriers that are coated with a randomly surface-textured transparent conductive oxide (TCO) layer. In this letter we introduce a model that relates the surface morphology of a thin film to its scattering properties. Such a model can help understanding the scattering properties of rough surfaces and contribute to optimizing the surface morphologies of the TCO layers for enhanced scattering.

The root mean square (rms) roughness σ_r and the height function $\eta(x,y)$ are used to describe the surface morphology of a rough surface. The far field of the scattered light is described by two parameters. The haze parameter $H(\lambda)$ is given by the ratio of the scattered light to the total light and can be defined for both transmitted and reflected lights. The angular intensity distribution $I(\theta,\lambda)$, where θ is the scattering angle [see Fig. 1(a)], is given by the magnitude of the Poynting vector.

To find mathematical relations between the surface morphology parameters σ_r and $\eta(x,y)$ and the far field parameters $H(\lambda)$ and $I(\theta,\lambda)$, the scalar scattering theory can be used. Based on this theory, several models have been introduced to calculate the haze parameters of reflected and transmitted light as a function of σ_r.[2–6] In this letter, we present a model that predicts the *angular* intensity distribution $I(\theta,\lambda)$ of the scattered light, using the height function $\eta(x,y)$ of the rough surface as input parameter. In this way also the lateral features of the rough surface are taken into account.

In the scalar scattering theory the complex vectors of the electromagnetic field, $\mathbf{H}(\mathbf{r},\omega)$ and $\mathbf{E}(\mathbf{r},\omega)$, at a position $\mathbf{r}$ are replaced by a complex scalar field $U(\mathbf{r},\omega)$. The angular frequency ω is connected to the wavelength via $\lambda=(2\pi c)/[n(\omega)\omega]$, where n is the refractive index. The normalized intensity $\mathcal{I}=I/I_0$, where I_0 is the intensity of the incident light, is given by $\mathcal{I}=|U|^2$.

Let now $U^{\text{inc}}=\exp(ik\mathbf{s}_0\mathbf{r})$ be a monochromatic incident plane wave, propagating along the direction $\mathbf{s}_0$ and with the wave vector $k=2\pi/\lambda$ as illustrated in Fig. 1(a). If U^{inc} is scattered by a rough surface of a thin film that covers the volume V, the scattered field U^{sca} far away from the film, i.e., if $kr\to\infty$, can be written as

$$U^{\text{sca}}(r\mathbf{s},\omega)=f(\mathbf{s},\mathbf{s}_0;\omega)\frac{1}{r}e^{ikr}, \tag{1}$$

where the position is given by $r\mathbf{s}=\mathbf{r}$ and the unit vector $\mathbf{s}$ denotes the direction. The function f is called *scattering amplitude*. It is given by

$$f(\mathbf{s},\mathbf{s}_0;\omega)=\iiint_V F(\mathbf{r}',\omega)U(\mathbf{r}',\omega)e^{-ik\mathbf{s}\mathbf{r}'}d^3r', \tag{2}$$

where U is the field inside the volume. F is the *scattering potential* that is defined as

$$F(\mathbf{r},\omega)=\frac{1}{4\pi}k^2[n^2(\mathbf{r},\omega)-1]. \tag{3}$$

If we assume that light is only scattered once at the rough surface, we may write $U(\mathbf{r},\omega)\approx U^{\text{inc}}(\mathbf{r},\omega)=\exp(ik\mathbf{s}_0\mathbf{r})$ if $\mathbf{r}\in V$. This assumption applied to Eq. (2) leads to the *first order Born approximation*,

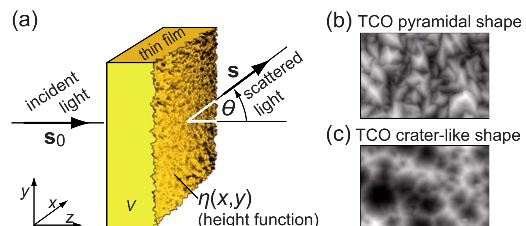

FIG. 1. (Color online) Illustrating scattering at a thin film with one roughly textured surface (a), and indicating a pyramidal (b) and a craterlike (c) TCO surface structure.

a)Electronic mail: k.jaeger@tudelft.nl.

 © 2009 American Institute of Physics

Downloaded 06 Aug 2010 to 131.180.130.114. Redistribution subject to AIP license or copyright; see http://apl.aip.org/apl/copyright.jsp

$$f_1(\mathbf{s},\mathbf{s}_0) = \iiint_V F(\mathbf{r}')e^{-i\mathbf{K}\mathbf{r}'}d^3r', \tag{4}$$

where $\mathbf{K}=k(\mathbf{s}-\mathbf{s}_0)$. The scattering amplitude f_1 therefore is given by the three-dimensional Fourier transform of the scattering potential F.

We assume n, and thus F, to be constant over the volume of the thin film, i.e., $F(\mathbf{r},\omega)\equiv F(\omega)$. After integrating Eq. (4) over z, we find

$$f_1 = F\iint_A \mathcal{Z}\exp[-i(K_x x + K_y y)]dxdy, \tag{5}$$

where A is along the rough surface of the thin film and

$$\mathcal{Z} = \frac{1}{iK_z}\{1-\exp[-iK_z\eta(x,y)]\}. \tag{6}$$

We note that $\mathcal{Z}$ contains the height function $\eta(x,y)$ that is the input parameter for our model.

To calculate K_z we recall that the light hits the obstacle along the z-axis and $\mathbf{s}_0$ thus only has a z-component of $s_{0,z}=1$. Due to the unity of $\mathbf{s}$ we therefore obtain

$$K_z = k(\sqrt{1-s_x^2-s_y^2}-1). \tag{7}$$

If we assumed $\mathcal{Z}\equiv 1/ik$ in Eq. (5), we would obtain, up to a constant, the Fraunhofer equation for scattering at an opening A (see, e.g., Ref. 7, Sec. 8.3.3).

The scattering angles θ, as in Fig. 1(a), are given by

$$\sin\,\theta = \frac{1}{k}\sqrt{K_x^2+K_y^2}. \tag{8}$$

$\theta=0°$ corresponds to the direction of the incoming light. The Fourier components with $K_x^2+K_y^2>k^2$ correspond to the evanescent field of the scattered light that is not observed in the far field region.

Since we are interested in the normalized intensity of the scattered light, the phase $\exp(ikr)$ in Eq. (1) may be neglected. To match the calculated with the measured normalized values, we introduce the factor A_{opt}/A, where the area A_{opt} is dependent on the optical measurement system. By taking Lambert's cosine law into account we thus obtain for the normalized intensity of the scattered light,

$$\mathcal{I}(\lambda,\theta) = \frac{A_{\text{opt}}}{A}\cos\,\theta\left|\frac{F}{r}\iint_A \mathcal{Z}e^{-i(K_x x+K_y y)}dxdy\right|^2. \tag{9}$$

To validate the model, we used four different glass-TCO samples each having a different surface morphology. We determined the TCO surface parameters that served as the input for the model, $\eta(x,y)$ and σ_r, with an NT-MDT NTEGRA atomic force microscope (AFM) in noncontact mode. The AFM measurements were carried out with gold coated silicon cantilevers on areas between $A=10\times 10\ \mu\text{m}^2$ and $A=50\times 50\ \mu\text{m}^2$ taking 256×256 points. To determine $\mathcal{I}(\lambda,\theta)$, we used variable angle spectrometry (VAS), which was carried out in the analytical reflectance/transmittance analyzer (ARTA) setup.[8] The ARTA setup measures the $\mathcal{I}(\lambda,\theta)$ both as a function of the scattering angle and the wavelength. The wavelength was varied between $\lambda=300$ and 800 nm. Since the light is incident normal to the glass substrate [see Fig. 1(a)], the influence of the glass on the scattering behavior of the rough TCO surface can be neglected.

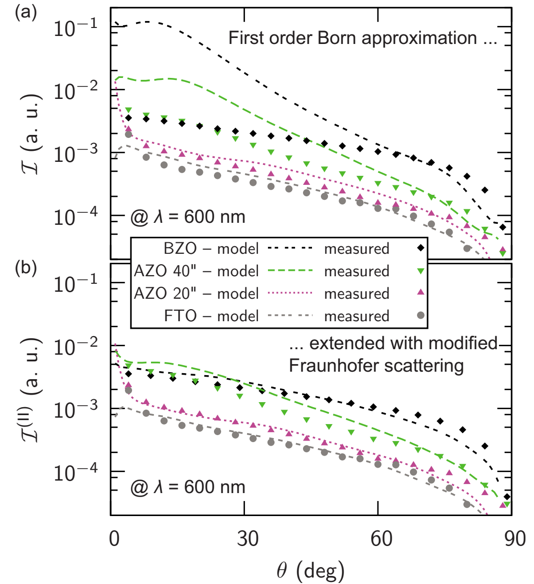

FIG. 2. (Color online) Measurements and the application of Eq. (9) with the first order Born approximation, $\mathcal{Z}$ [Eq. (6)], (a) and a modified Fraunhofer scattering extension, $\mathcal{Z}^{(\text{II})}$ [Eq. (10)], (b) are shown for four samples at $\lambda=600$ nm.

The distance between the sample and the detector was $r=9$ cm.

Figures 1(b) and 1(c) illustrate the surface morphologies of the samples. Fluorine-doped tin oxide (FTO) of Asahi U-type prepared using atmospheric pressure chemical vapor deposition shows a pyramidal structure[9] and is characterized by $\sigma_r\approx 40$ nm. Sputtered aluminum-doped zinc oxide (AZO) that is etched in a 0.5% HCl solution shows a craterlike structure.[10] One can change σ_r by varying the etching time. In this study we deal with AZO of 20″ and 40″ etching time and $\sigma_r\approx 50$ and $\sigma_r\approx 100$ nm, respectively. Low-pressure chemical vapor deposited boron-doped zinc oxide (BZO) of type B from the PV-LAB of the École polytechnique fédérale de Lausanne (EPFL), Switzerland shows a pyramidal structure[11] and has $\sigma_r\approx 220$ nm.

We evaluated the scattered light only and did not take the specular peak around $\theta=0°$ into account. We applied an averaging and smoothing method in order to reduce noise. We used the approximation $n(\lambda)\equiv 2$ and calibrated the model with $A_{\text{opt}}=6\times 10^{-5}$ m^2, where A_{opt} is as in Eq. (9). The calculations led to the same results for AFM scan areas between $A=10\times 10\ \mu\text{m}^2$ and $A=50\times 50\ \mu\text{m}^2$. The results discussed in the following paragraphs were obtained with $A=20\times 20\ \mu\text{m}^2$ scans.

Figure 2(a) shows measured and simulated normalized angular intensity distributions of the four samples at $\lambda=600$ nm. Good agreement is achieved for FTO ($\sigma_r\approx 40$ nm) and for AZO 20″ ($\sigma_r\approx 50$ nm). However, for AZO 40″ ($\sigma_r\approx 100$ nm) and BZO ($\sigma_r\approx 220$ nm) large deviations between the measured and calculated intensities are observed. This is because the first order Born approximation only works for samples with a moderate rms roughness.[12] If σ_r is small compared to the wavelength, i.e., if the condition $k\sigma_r\ll 1$ is fulfilled, we can approximate $\mathcal{Z}$ [Eq. (6)] with $\mathcal{Z}^{(\text{I})}=\eta(x,y)$, which allows us to evaluate Eq. (9) with fast Fourier transform algorithms. The application of $\mathcal{Z}^{(\text{I})}$ led to results similar to those already shown in Fig. 2(a).

Downloaded 06 Aug 2010 to 131.180.130.114. Redistribution subject to AIP license or copyright; see http://apl.aip.org/apl/copyright.jsp

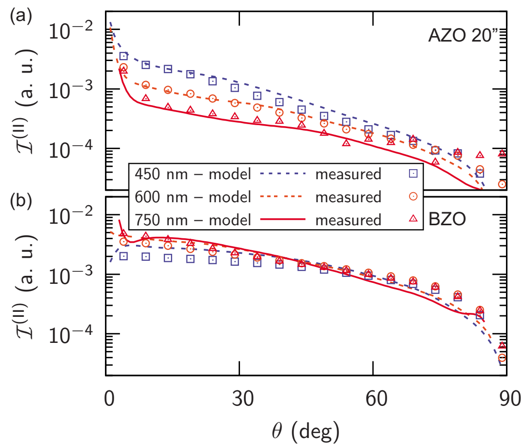

FIG. 3. (Color online) Measurements and model, extended with modified Fraunhofer scattering, for AZO 20″ (a) and BZO (b) at three different wavelengths.

In order to obtain better matching between measured and calculated intensities for large values of σ_r, we modified Eq. (9) by replacing $\mathcal{Z}$ [Eq. (6)] with

$$\mathcal{Z}^{(\mathrm{II})} = \frac{1}{ik}\{1 - \exp[-ik\eta(x,y)]\}, \tag{10}$$

which can be interpreted as *modified Fraunhofer scattering* (see, e.g., Ref. 7, Sec. 8.3.3). A phase shift $1-\exp[-ik\eta(x,y)]$ in Eq. (10) contains the surface data. Since in Eq. (10) K_z is replaced by k, fast Fourier transform algorithms can be used to evaluate Eq. (9). Results are shown in Fig. 2(b). While for FTO and AZO 20″ we hardly observe any difference between Figs. 2(a) and 2(b), the measured and calculated intensities for AZO 40″ and BZO match much better using the modified Fraunhofer scattering approach. However, for AZO 40″ the model overestimates the measured values.

Until now we only discussed the application of the model at one wavelength ($\lambda=600$ nm). Figure 3 shows the application of the first order Born approximation extended with the modified Fraunhofer scattering approach, which we already discussed in Fig. 2(b), for three different wavelengths to AZO 20″ ($\sigma_r \approx 50$ nm) and BZO ($\sigma_r \approx 220$ nm). For AZO 20″, the trend that scattering at shorter wavelengths leads to higher intensities is reproduced in the correct way. Also for BZO, the model predicts the trends correctly.

We applied the first order Born approximation to relate the angular intensity distribution of light that is scattered by roughly textured thin films to their surface morphology. We obtained good agreement between the calculated and measured angular intensity distribution for textures with a rms roughness between $\sigma_r=40$ nm and 50 nm. The extension of the model with a modified Fraunhofer scattering approach is needed to obtain good agreement for samples with $\sigma_r \geq 100$ nm.

This work was carried out with funding from Nuon Helianthos. The authors would like to thank Janez Krč from the University of Ljubljana and Rudi Santbergen and Omar El Gawhary from the Delft University of Technology for the stimulating discussions. We acknowledge Zhao Lu for carrying out the VAS measurements and the PV-LAB of the EPFL, Switzerland, for supplying us with BZO samples.

[1] H. W. Deckman, C. R. Wronski, H. Witzke, and E. Yablonovitch, Appl. Phys. Lett. **42**, 968 (1983).
[2] H. Stiebig, T. Brammer, T. Repmann, O. Kluth, N. Senoussaoui, A. Lambert, and H. Wagner, Proceedings of the 16th European Photovoltaic Solar Energy Conference, Glasgow, UK, May 2000 (unpublished), p. 549.
[3] M. Zeman, R. A. C. M. M. van Swaaij, J. W. Metselaar, and R. E. I. Schropp, J. Appl. Phys. **88**, 6436 (2000).
[4] J. Krč, M. Zeman, F. Smole, and M. Topič, J. Appl. Phys. **92**, 749 (2002).
[5] J. Krč, M. Zeman, O. Kluth, F. Smole, and M. Topič, Thin Solid Films **426**, 296 (2003).
[6] J. Springer, A. Poruba, and M. Vanecek, J. Appl. Phys. **96**, 5329 (2004).
[7] M. Born and E. Wolf, *Principles of Optics*, 7th ed. (Cambridge University Press, Cambridge, 1999).
[8] P. A. van Nijnatten, Thin Solid Films **442**, 74 (2003).
[9] K. Sato, Y. Gotoh, Y. Wakayama, Y. Hayashi, K. Adachi, and N. Nishimura, Rep. Res. Lab.: Asahi Glass Co. Ltd. **42**, 129 (1992).
[10] M. Berginski, J. Hüpkes, M. Schulte, G. Schöpe, H. Stiebig, B. Rech, and M. Wuttig, J. Appl. Phys. **101**, 074903 (2007).
[11] D. Dominé, P. Buehlmann, J. Bailat, A. Billet, A. Feltrin, and C. Ballif, Phys. Status Solidi (RRL) **2**, 163 (2008).
[12] F. Simonetti, Phys. Rev. E **73**, 036619 (2006).

Downloaded 06 Aug 2010 to 131.180.130.114. Redistribution subject to AIP license or copyright; see http://apl.aip.org/apl/copyright.jsp